Available online at www.sciencedirect.com
SCIENCE DIRECT
Geochimica et Cosmochimica Acta 70 (2006) 1849–1863
Geochimica
www.elsevier.com/locate/gca

Determination of the petrologic type of CV3 chondrites by Raman spectroscopy of included organic matter

Lydie Bonal [a,*], Eric Quirico [a], Michèle Bourot-Denise [b], Gilles Montagnac [c]

[a] *Laboratoire de Planétologie de Grenoble, Université Joseph Fourier, Observatoire des Sciences de l'Univers de Grenoble (OSUG), Bât. D de Physique, BP 53, 38041 Grenoble Cedex 9, France*
[b] *Museum National d'Histoire Naturelle, Laboratoire d'Etude de la Matière Extraterrestre, 61 rue Buffon, 75231 Paris Cedex 05, France*
[c] *Laboratoire de Sciences de la Terre ENS Lyon, 46, allée d'Italie, 69364 Lyon Cedex 7, France*

Received 11 February 2005; accepted in revised form 9 December 2005

Abstract

This paper reports the first reliable quantitative determination of the thermal metamorphism grade of a series of nine CV3 chondrites: Allende, Axtell, Bali, Mokoia, Grosnaja, Efremovka, Vigarano, Leoville, and Kaba. The maturity of the organic matter in matrix, determined by Raman spectroscopy, has been used as a powerful metamorphic tracer, independent of the mineralogical context and extent of aqueous alteration. This tracer has been used along with other metamorphic tracers such as Fe zoning in type-I chondrules of olivine phenocrysts, presolar grain abundance and noble gas abundance (bulk and P3 component). The study shows that the petrologic types determined earlier by Induced ThermoLuminescence were underestimated and suggests the following values: PT (Allende-Axtell) >3.6; PT (Bali-Mokoia-Grosnaja) ~3.6; PT (Efremovka-Leoville-Vigarano) = 3.1–3.4; PT (Kaba) ~3.1. The most commonly studied CV3, Allende, is also the most metamorphosed. Bali is a breccia containing clasts of different petrologic types. The attribution suggested by this study is that of clasts of the highest petrologic types, as pointed out by IOM maturity and noble gas bulk abundance. CV3 chondrites have complex asteroidal backgrounds, with various degrees of aqueous alteration and/or thermal metamorphism leading to complex mineralogical and petrologic patterns. (Fe,Mg) chemical zoning in olivine phenocrysts, on the borders of type I chondrules of porphyritic olivine- and pyroxene-rich textural types, has been found to correlate with the metamorphism grade. This suggests that chemical zoning in some chondrules, often interpreted as exchanges between chondrules and nebular gas, may well have an asteroidal origin. Furthermore, the compositional range of olivine matrix is controlled both by thermal metamorphism and aqueous alteration. This does not support evidence of a nebular origin and does not necessarily mirror the metamorphism grade through (Fe,Mg) equilibration. On the other hand, it may provide clues on the degree of aqueous alteration vs. thermal metamorphism and on the timing of both processes. In particular, Mokoia experienced significant aqueous alteration after the metamorphism peak, whereas Grosnaja, which has similar metamorphism grade, did not.

1. Introduction

Chondritic meteorites provide essential information on the conditions that prevailed in the early solar system. Nevertheless, nebular or presolar records may have been obscured or completely erased by secondary processes in the parent body (e.g., thermal metamorphism and/or aqueous alteration). One of the major goals in the study of chondrites is to quantify their degree of primitiveness to select the most relevant objects for early Solar System studies. CV carbonaceous chondrites are characterised by the most abundant and largest refractory inclusions (Calcium–Aluminium-rich inclusions), which contain precious chronological and irradiation event information. In the first general paper devoted to CV chondrites, McSween (1977) characterised them as a very heterogeneous and complex class of meteorites. He noted their considerable mineralogical, petrologic, and chemical diversity in comparison with CO3 chondrites. McSween (1977) first provided evidence of

* Corresponding author.
E-mail address: lydie.bonal@obs.ujf-grenoble.fr (L. Bonal).

0016-7037/$ - see front matter © 2005 Elsevier Inc. All rights reserved.
doi:10.1016/j.gca.2005.12.004

different degrees of aqueous alteration and divided the CV3 class into the so-called reduced and oxidised subgroups, according to the abundance of metallic Fe–Ni phases vs. magnetite, and to the Ni content in sulphides. The oxidised subgroup was later divided into two subgroups: Allende-like chondrites ($CV3_{OxA}$) and Mokoia-like chondrites ($CV3_{OxB}$) (Weisberg et al., 1997). More recent evidence relates aqueous alteration to the presence of phyllosilicates (Keller and Buseck, 1990; Tomeoka and Buseck, 1990; Keller and McKay, 1993; Keller et al., 1994; Tomeoka and Tanimura, 2000).

Evidence of thermal metamorphism is less clear. The question of the metamorphic grade of CV3 chondrites was investigated by Guimon et al. (1995), using the Induced ThermoLuminescence (ITL) technique generally applied to unequilibrated ordinary chondrites (UOCs). This study suggests that CV3 chondrites are systematically of low metamorphic grade with a maximum petrographic type (PT) of 3.3 for a series of 14 CV3s. These results are however not consistent with the study by McSween (1977) who suggested that Allende had experienced significant metamorphism. Other recent petrologic evidence indicates that Allende is more metamorphosed than Bali and thermal metamorphism could largely explain the difference between these objects by the decomposition of phyllosilicates and the formation of minerals like nepheline and sodalite (Krot et al., 1997). Furthermore, the petrologic types derived by Guimon et al. (1995) are not consistent with noble gas data in presolar grains (Huss et al., 1996) or with the maturation grade of organic matter (OM) (Quirico et al., 2003). The latter study suggests that Allende and Axtell would be better described by a type of at least 3.6.

One of the major questions concerning CV3 chondrites is whether they contain petrologic evidence of nebular records in chondrules and matrix, or whether this evidence is indeed the result of asteroidal process. This question has long been debated. It has been suggested that chemical zoning in chondrules and fayalite grains in matrix are the result of nebular exchange or condensation (e.g., Peck and Wood, 1987; Weinbruch et al., 1994; Hua and Buseck, 1995; Ikeda and Kimura, 1996; Kimura and Ikeda, 1997; Weisberg and Prinz, 1998). On the other hand, Housley and Cirlin (1983), Housley (1986), Krot et al. (1995, 1998), and Kojima and Tomeoka (1996) favour asteroidal processes. Note that the conclusions of Krot et al. (1995) are the result of an extensive review of all work published before 1995.

A better understanding of the effect of asteroidal processes on the mineralogic composition and the petrology of CV3 chondrites would certainly help resolve this question. The goal of the present study is to determine the metamorphic grade of a series of nine CV3 chondrites belonging to both oxidised (Allende, Axtell, Bali, Mokoia, Grosnaja, and Kaba) and reduced (Efremovka, Leoville, and Vigarano) subgroups. Because CV3 may have experienced both a high degree of metamorphism grade and aqueous alteration, mineralogic tracers currently used may no longer be valid (e.g., compositional range of olivine grains in matrix). For this reason, we have used an approach based on the maturation grade of organic matter (OM). The principle of such an approach is that thermal metamorphism induces some irreversible structural, textural and compositional transformations in OM. Quantifying the degree of advancement in the carbonisation/graphitisation process may then provide the metamorphism grade experienced by the whole object (Quirico et al., 2003). We have also studied the chemical zoning in olivine phenocrysts, induced by Fe–Mg interdiffusion through equilibration. We have focused on olivine crystals in type I chondrules, of porphyritic olivine- and pyroxene-rich (POP) textural types. Raman and petrographic data have been compared with various metamorphic tracers available in the literature such as abundance of presolar grains (Huss and Lewis, 1995) and noble gases (Huss and Lewis, 1994a,b; Scherer and Schultz, 2000), and also with ITL results (Guimon et al., 1995).

2. Experimental

Raw samples and polished or thin sections were provided by several institutes (Table 1). To perform Raman measurements on matrix, millimetre-sized raw samples of each meteorite were crushed and several fresh matrix grains carefully selected among the fragments, under a binocular microscope, according to colour and texture. The selected matrix grains were crushed between two glass slides that were also used as the Raman substrate for the analysis. This procedure allowed us to work on fresh samples and enhance heat dissipation, thereby avoiding thermal damage.

Raman experiments were performed at Laboratoire de Sciences de la Terre (ENS-Lyon, France) with a LABRAM spectrometer (Horiba Jobin-Yvon). An excitation wavelength of 514.5 nm was used on a Spectra Physics argon ion laser. The laser beam was focused by a microscope equipped with a 50× objective, leading to a spot diameter

Table 1
Basic characteristics of the studied CV3s

Name	Oxidised/reduced	Fall/*find*
Allende[a,e]	O	Fall
Axtell[a,e]	O	*find*
Grosnaja[b, d, e]	O	Fall
Mokoia[a,b]	O	Fall
Bali[d,a]	O	Fall
Kaba[b,d]	O	Fall
Efremovka[a,c,e]	R	*find*
Leoville[a,c, e]	R	*find*
Vigarano[c,e]	R	Fall

Raw samples and sections were supplied by:
[a] Museum National d'Histoire Naturelle (Paris).
[b] British Museum (London).
[c] US National Museum of Natural History (Washington).
[d] Naturhistorisches Museum (Vienna).
[e] Field Museum of Natural History (Chicago).

of 2–3 μm. Experiments were performed under strictly constant experimental conditions: the power at the sample surface was 515 ± 5 μW and the acquisition time was 540 s. Under such conditions, thermal damage and heating were avoided and a visual check on the absence of any burial print was carried out after each acquisition. A minimum of 10 spectra was acquired for each chondrite in the spectral region 700–3700 cm^{-1}.

The petrographic study was performed using a Scanning Electron Microscope: BSE images of the chondrules were made using a JEOL JSM 840 A SEM at University Paris VI. Some profiles across the matrix–chondrule border were obtained using the SX100 electron μprobe of University Paris VI. Analyses of the silicates were carried out at 15 kV and 15 nA with the PAP program.

3. Raman spectra analysis

Raman spectroscopy is very sensitive to the degree of structural order of polyaromatic OM. The typical Raman spectrum of such a material exhibits several bands, the most intense being the first order band peaking at ~1600 cm^{-1} (G-band) and ~1350 cm^{-1} (D-band) (Fig. 1). The G-band (G for graphite) is assigned to the E_{2g2} vibrational mode of the aromatic plane and is present in all OM whatever the degree of structural order. On the other hand, the D-band (D for defects) is not present in a perfectly stacked graphite and is induced by structural defects in the material (e.g., Tuinstra and Koenig, 1970; Ferrari and Robertson, 2000). The only structural parameter which has been linked to the D- and G-band spectral parameters is the lateral size of the basic structural units of polyaromatic matter (e.g., Tuinstra and Koenig, 1970; Wopenka and Pasteris, 1993). Unfortunately, the available relationship is highly inaccurate for poorly ordered OM and in particular cannot be used to study chondritic OM. Nevertheless, some spectral parameters (referred to below as *maturity tracers*) are very sensitive to the degree of structural order of poorly ordered materials, although they do not provide quantitative structural information. Studies on series of coals and other natural sedimentary organic matter have provided different sets of parameters that correlate well with the maturation grade as quantified by vitrinite reflectance, for instance the width of the D-band (Wopenka and Pasteris, 1993; Kelemen and Fang, 2001; Quirico et al., 2005).

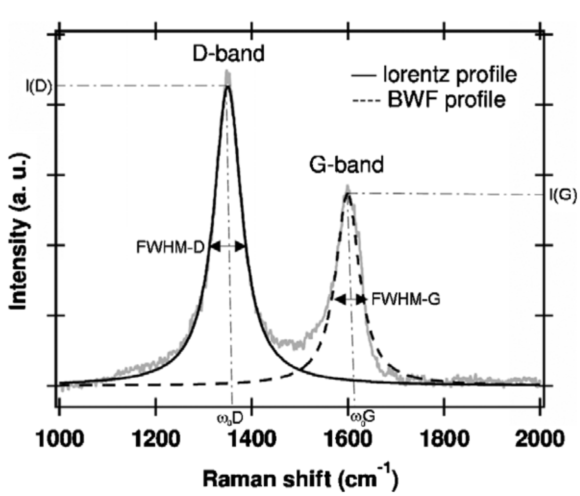

Fig. 1. Raman spectra of a polyaromatic carbonaceous material, intensity in arbitrary unit (a.u.). The D-band was fitted by a Lorenztian profile and the G-band by a Breit-Wigner-Fano profile to obtain the spectral parameters FWHM-D, FWHM-G, I_D, I_G, ω_0D, ω_0G.

The interpretation of the degree of structural order in terms of metamorphic grade for a series of samples requires (1) chemically and structurally similar organic precursors and (2) similar metamorphic conditions (time, pressure, etc.). If these two requirements are fulfilled, it is possible to derive a metamorphic hierarchy for the samples and in some cases provide the temperature of the metamorphism peak (Beyssac et al., 2002). On the other hand, Raman data may show differences in the organic precursor and are finally of help when testing the first requirement above (e.g., Beny-Bassez and Rouzaud, 1985). In particular, Quirico et al. (2003) have shown that terrestrial coals are not valid analogues of polyaromatic OM in unequilibrated ordinary chondrites.

In the present study, the analysis and interpretation of the Raman spectra follow those described by Quirico et al. (2003, 2005). The reproducibility of the measurements depends on the experimental parameters: acquisition time, power on the sample and atmospheric conditions. The effect of sample heating by laser irradiation is a crucial issue in Raman microscopy and has been extensively investigated. Heat-induced band shifts were observed more than one decade ago in graphitic materials (e.g., Everall et al., 1991 and references therein) and the accuracy and reproducibility of measurements has been studied by many authors (e.g., Everall et al., 1991; Beyssac et al., 2003). For less organised polyaromatic materials such as coals or chondritic OM, the effect of laser irradiation is more complicated as photo-oxidation processes play a key role (e.g., Pradier et al., 1992). These processes control not only the variations of the fluorescence intensity as a function of time, but probably also those of the spectral parameters of the G- and D-bands, raising the question of measurement reproducibility (Quirico et al., 2005). Optimum measurement conditions are obtained in an inert atmosphere, minimising photo-oxidation and ensuring good reproducibility. Another approach is to perform experiments with strictly constant acquisition times and power on the sample surface. This second approach has been used as it facilitates cross-measurements between different laboratories.

Having dealt with reproducibility, the accuracy of the spectral maturity tracers must be considered. The tracers used in this study (see below) were earlier derived from measurements on only five coals with a maturity consistent with that of type 3 chondrites (Quirico et al., 2003). A larger number of coals must be used. Moreover, the Raman spectrometer used in this study was more sensitive than the one used by Quirico et al. (2003) and allowed spectra acquisition over a wider spectral range (700–3700 vs. 1070–1790 cm^{-1}). In the spectra acquired for this study, a baseline correction was applied between 700 and 2000 cm^{-1}. As discussed below, the spectral parameters are sensitive to the baseline correction, making quantitative comparison of earlier and present data impossible.

Consequently measurements were carried out under strictly constant experimental conditions and data processing procedures were performed on (1) the series of UOCs explored by Quirico et al. (2003) supplemented by the Parnallee chondrite (LL3.7) ; (2) an extended series of coals (7 more than in the previous study), used as comparison standards, with 1.16% < VR < 7.02% (VR: vitrinite reflectance) and (3) the series of nine CV3 chondrites.

3.1. Fitting procedure

All spectra exhibit the first and second order carbon bands. The analysis here was focused on the G- and D-bands of the first order. First, the fluorescence background was subtracted assuming a linear baseline between 700 and 2000 cm^{-1}. Next, the G- and D-bands were fitted with two spectral profiles (LBWF fit): a Lorentzian (L) profile for the D-band and a Breit-Wigner-Fano (BWF) profile for the G-band. In Quirico et al. (2003), this fit was applied to high-rank coals while a 2-Lorentzian fit was preferred for samples with lower maturities (including the Semarkona chondrite). However, we have performed systematic studies that have shown that the LBWF model better fits the Raman spectra of all kind of samples, whatever their maturity. The 2-Lorentzian fit is therefore not used. The LBWF fitting was performed with the IDL software (from Research Systems) using the Curvefit procedure. The following spectral parameters were derived for each spectrum: peak position $\omega_{D,G}$, peak intensity $I_{D,G}$, integrated intensity $A_{D,G}$ and Full Width at Half Maximum FWHM-D, G (Fig. 1). The final parameters used to quantify the maturity were FWHM-D, FWHM-G, ω_D, ω_G, I_D/I_G and $A_D/[A_D + A_G]$. For each coal, the mean value and the standard deviation (σ) of each of these parameters have been calculated over 15 spectra.

3.2. Definition of the spectral maturity tracers

Eleven coals with vitrinite reflectance (VR) ranging between 1% and 7% have been measured (Table 2). The Raman spectral parameters are presented in the so-called G (FWHM-G vs. ω_G), D (FWHM-D vs. ω_D) and DG (I_D/I_G vs. $[A_D]/[A_D + A_G]$) diagrams (Fig. 2). The most sensitive spectral maturity tracers are the width of the D-band and the ratio of the peak intensities of the D- and G-bands for our range of maturity (Quirico et al., 2005). Thus, the most useful tracers for the present study, FWHM-D and I_D/I_G, are plotted along with VR for each rank of coals (Figs. 3a and b). The measurements confirm the general trends earlier reported: FWHM-D decreases with increasing maturity and I_D/I_G decreases for VR $\leqslant$ 5% and then increases. Nevertheless, certain amendments are required for the quantitative use of these spectral parameters. First, the range of validity of FWHM-D as a maturity tracer appears smaller here as it does not correlate with VR between 1% and 2.0%. Between 2.5% and 7%, the variations of FWHM-D are large (90–230 cm^{-1}) regarding the global range of variations and the 1σ dispersion. This suggests that this parameter is useful, but that the derived maturities are not necessarily accurate and might even be misleading for objects with similar maturities. Thus for a more pertinent analysis, FWHM-D must be used in combination with the parameter I_D/I_G. In the range 5–7%, I_D/I_G is particularly sensitive to maturity (Fig. 3b). Consequently, FWHM-D and I_D/I_G are two complementary tracers that we have systematically used together.

Table 2
Coal samples studied[a]

COPL name	VR (%)	ASTM rank[b]
9350-4	7.02	Meta-anthracite
PSOC1468	5.45	Anthracite
DECS21	5.19	Anthracite
PSOC1515	2.80	Semi-anthracite
PSOC384	2.70	Semi-anthracite
PSOC383	2.57	Semi-anthracite
PSOC880	1.86	Low volatile bituminous
PSOC1516	1.73	Low volatile bituminous
PSOC1550	1.35	Medium volatile bituminous
PSOC1540	1.28	Medium volatile bituminous
DECS30	1.16	Medium volatile bituminous

[a] All samples originate from the Coal Sample Bank and Database (University of Pennsylvania, USA), except meta-anthracite, which was kindly provided by Dr. Gareth Mitchell. COPL name, denomination of the coals in the Coal Sample Bank and Database; VR (%), reflectance of the vitrinite maceral, indicating the maturation grade.

[b] The rank is given along with the ASTM classification (standard D-388).

The D and G diagrams exhibit a trend that is consistent with the results of Quirico et al. (2003). However, the DG diagram is different. According to the data of Quirico et al. (2003), $[A_D]/[A_D + A_G]$ increases as the coal rank decreases over the whole range of maturity, resulting in a U-pattern metamorphic pathway. Such a pattern is not observed in the new set of data. The mean parameters of the more mature coals are comparable, but the data of the less mature coals are not. Nevertheless, the differences observed between the new set of data and the data from Quirico et al. (2003) do not question the method applied in the maturation range of chondrites of petrologic type 3 and above. Indeed, differences between this study and that of Quirico et al. (2003) are mostly observed for the less mature coals; and the maturation grade of the chondritic OM is comparable with that of high-rank coals.

3.3. Measurements on a UOC series for cross-calibrations

The Unequilibrated Ordinary Chondrites studied are the same as those considered by Quirico et al. (2003): Semark-

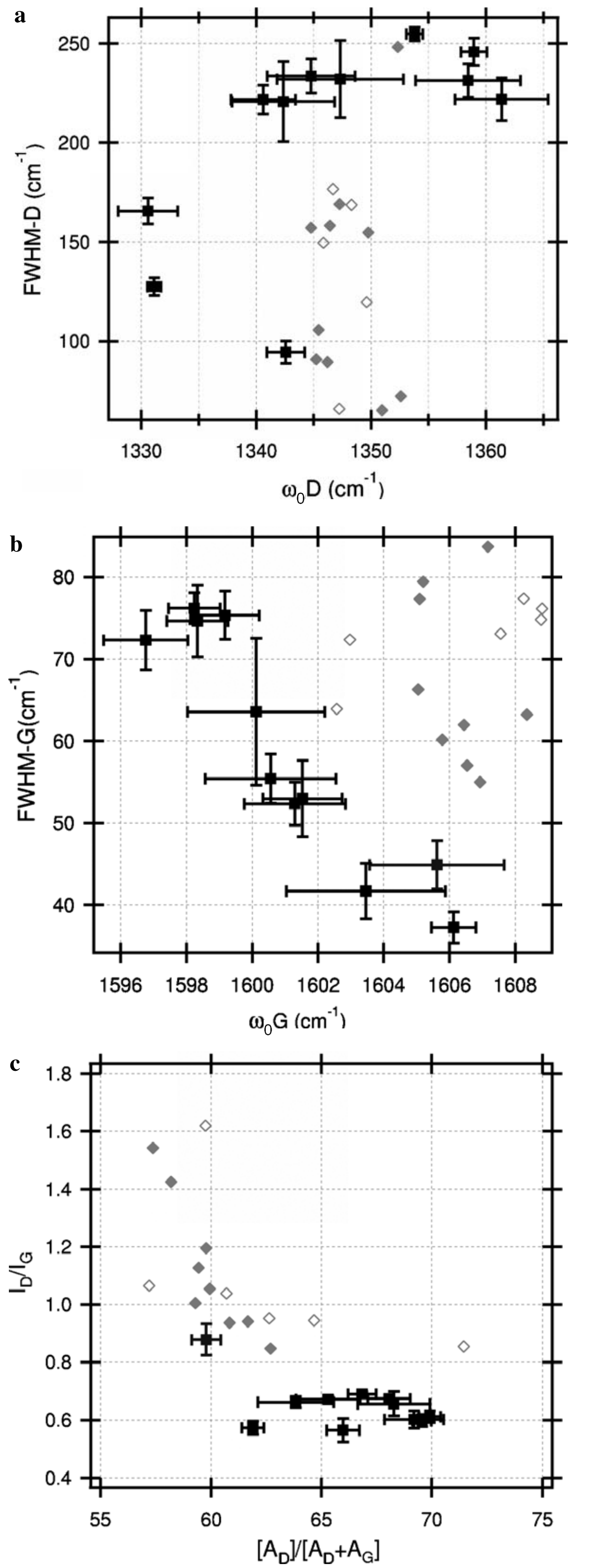

Fig. 2. Spectral parameters of Raman bands of carbonaceous materials in coal series. Averages of 15 spectra (points) and standard deviations (bars) are plotted. (a) D-diagram of FWHM-D vs. ω_D. (b) G-diagram of FWHM-G vs. ω_G. (c) DG-diagram of I_D/I_G vs. $[A_D]/[A_D + A_G]$.

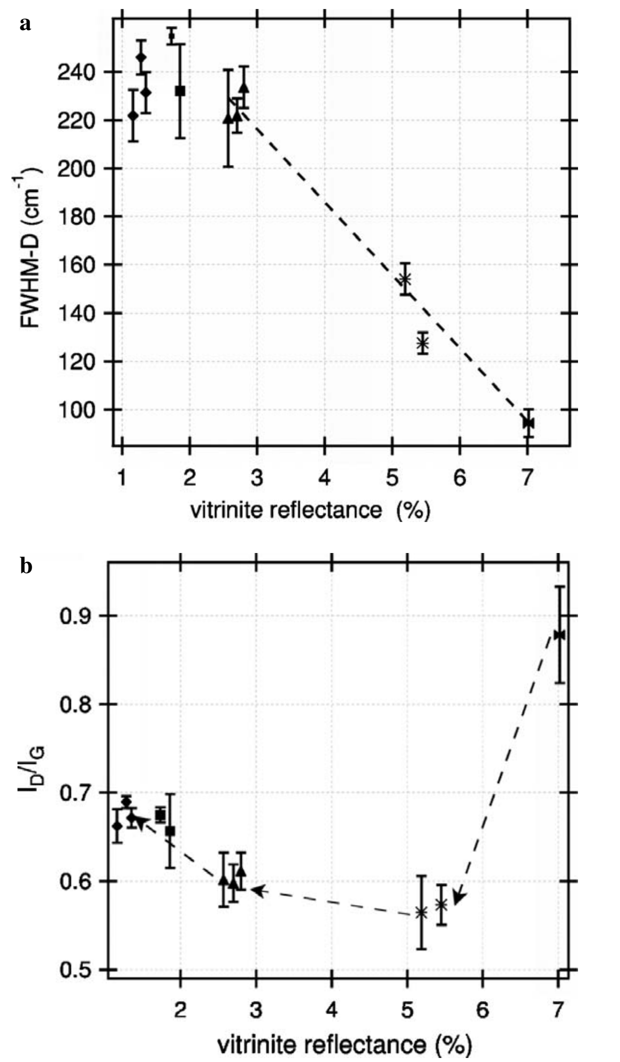

Fig. 3. Spectral parameters of Raman bands of carbonaceous materials in coal series vs. vitrinite reflectance. (a) Width of the D-band vs. the vitrinite reflectance VR% of the studied coals. Both these parameters are particularly well correlated for the anthracite series. FWHM-D appears to be a very accurate tracer of the metamorphic grade of these samples; (b) I_D/I_G vs. the vitrinite reflectance V% of the studied coals. The data points form a metamorphic pathway (grey arrows) between the different ranks of coals.

ona (LL3.0), Bishunpur (L/LL3.1), Krymka (LL3.1), Chainpur (LL3.4), and Tieschitz (H/L 3.6), supplemented by Parnallee (LL3.7). FWHM-D decreases with increasing maturity. In this series, FWHM-D distinguishes Semarkona from all others, Bishunpur and Krymka are very close, the first being slightly more mature than the second, and Chainpur, Tieschitz, and Parnallee can be plotted clearly in the maturity order Chainpur < Tieschitz < Parnallee. The maturities derived from I_D/I_G are consistent with those from FWHM-D (Fig. 4). These results show that both tracers are consistent and provide a reliable maturity hierarchy. They are thus suitable for studying the CV3 chondrites. Moreover, these results are consistent with those of Quirico et al. (2003), with a very good correlation between the Raman spectral parameter FWHM-D from Quirico et al.

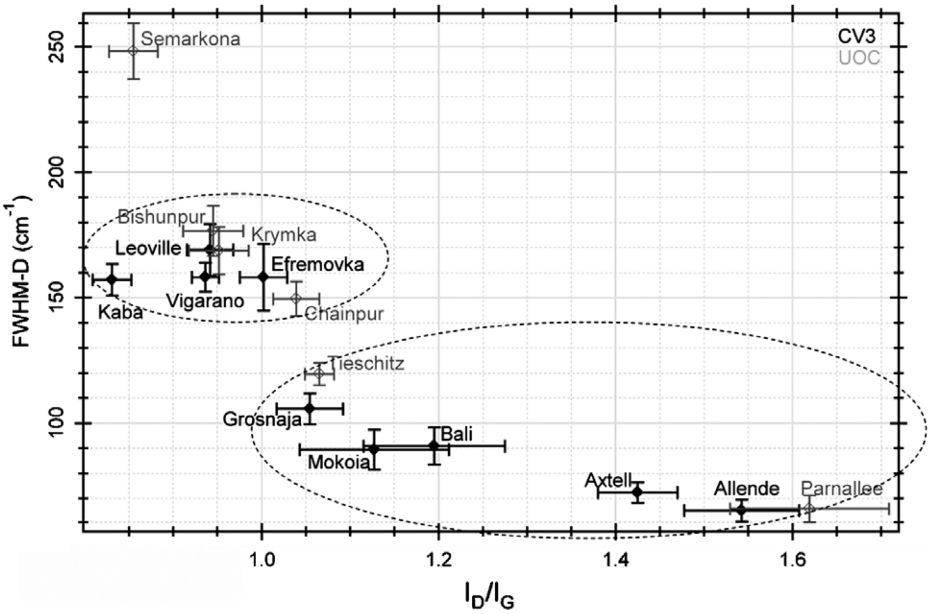

Fig. 4. Spectral parameters of Raman bands of carbonaceous materials in chondrite meteorites: FWHM-D vs. I_D/I_G. Averages (points) and standard deviations (bars) are plotted for Unequilibrated Ordinary Chondrites (grey dots) and for CV3 chondrites (black dots).

(2003) and the one from the present study. The two data sets are related by a simple factor of 0.88 (Fig. 5). Although the absolute values of the data set depend on the experimental conditions and numerical processing, the method provides a self-consistent set of measurements.

Nevertheless, two samples require further discussion. First, Quirico et al. (2003) observed an inversion in the relative classification of Krymka and Bishunpur, as indicated by both FWHM-D and I_D/I_G. In the present set of data, both tracers indicate that the OM of Bishunpur is less mature than that of Krymka. Krymka would therefore be less primitive than Bishunpur. This result is consistent with independent petrologic tracers: olivine compositional heterogeneities (Alexander et al., 1989) and also the loss of chromium from olivine, controlled by thermal metamorphism, indicating type 3.2 for Krymka (Grossman, 2004). Raman measurements from Quirico et al. (2003) probably suffered from an artefact, as the experimental conditions corresponding to the set of data were not controlled as strictly as in the present Raman measurements. Nevertheless, as discussed above, it is difficult to discriminate between objects with such similar OM maturities using this method. Second, the FWHM-D and I_D/I_G maturity tracers show significant differences between Parnallee (LL3.7) and Tieschitz (H/L3.6), suggesting a higher petrologic type for Parnallee (Fig. 4). This observation is indeed consistent with olivine zoning: SEM images of polished sections have shown that equilibrated olivines are visible in Parnallee, while none are found in Tieschitz. According to the thermoluminescence data, Sears et al. (1983) attributed type 3.6 to Parnallee, but the same authors (Sears et al., 1991b) subsequently proposed type 3.7. According to the present work, the petrologic type of Parnallee is underestimated, and should range between 3.7 and 3.8. In the following of this paper, Parnallee will be classified as a LL 3.7.

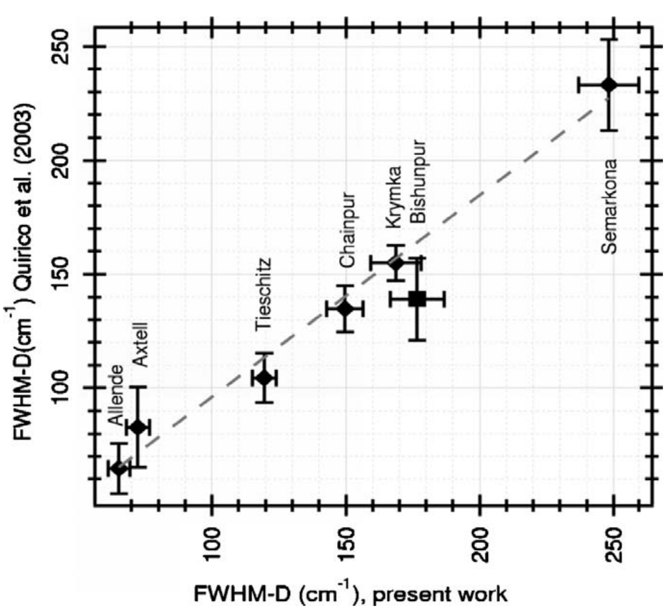

Fig. 5. Comparison of data obtained on UOCs by Quirico et al. (2003) and data obtained in this study using a well-defined experimental protocol. The dotted line shows good consistency between the two sets of data with a correlation coefficient of 0.88.

4. Results

4.1. Maturation grade of the organic matter

All spectra of the nine studied chondrites exhibit 1st order D- and G-bands (around 1350 cm^{-1} and 1580–1600 cm^{-1}, respectively). The intensity of the fluorescence background of the Raman spectra is weak. An initial visual examination of the raw spectra (Fig. 6) reveals significant differences between the samples. For Vigarano, Leoville, Kaba, and Efremovka, the peak intensity of the G-band

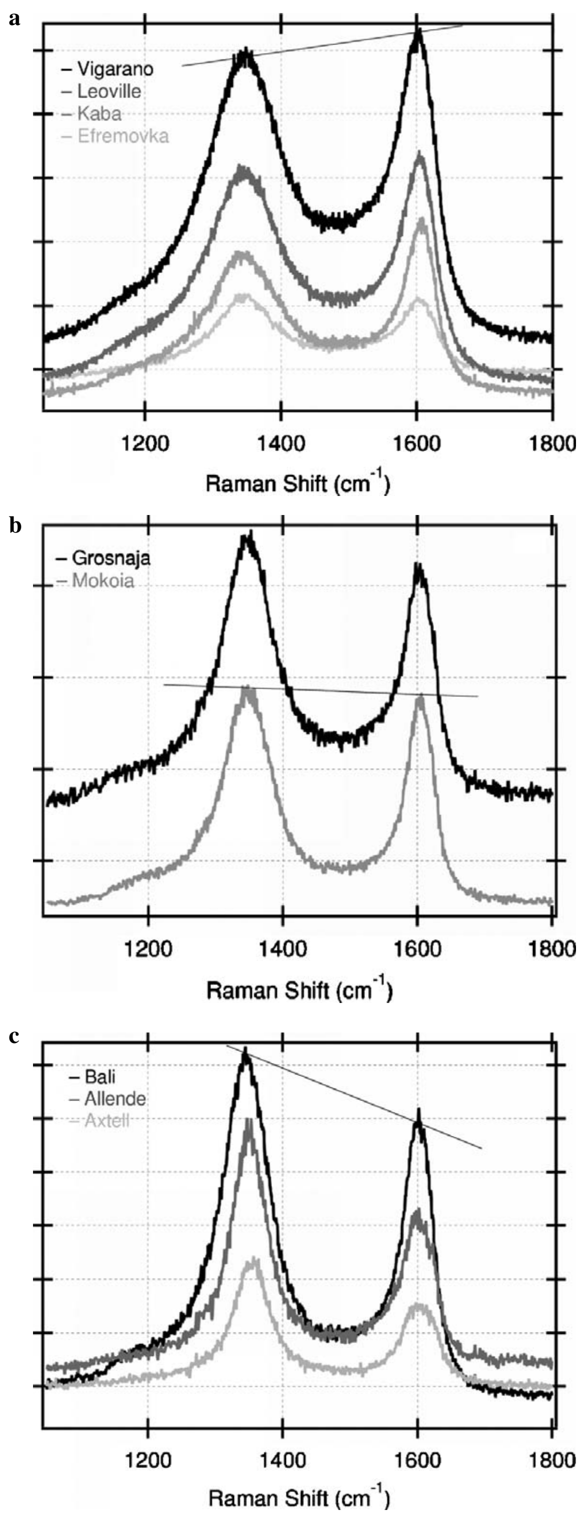

Fig. 6. Raw spectra of the CV3 chondrites. Differences are revealed in the structural state of the organic matter. (a) $I_D/I_G < 1$ for Efremovka, Leoville, Vigarano and Kaba. (b) $I_D/I_G \sim 1$ for Mokoia and Grosnaja. (c) $I_D/I_G > 1$ for Bali, Allende, and Axtell.

(I_G) is higher than that of the D-band (I_D). Both are roughly equal for Mokoia and Grosnaja, and $I_D > I_G$ for Bali, Allende, and Axtell. The width of the D-band tends to decrease with increasing I_D/I_G.

FWHM-D and I_D/I_G tracers depict two main groups (Fig. 4). The 1st group contains the less mature objects, i.e., Kaba, Vigarano, Leoville, and Efremovka characterised by FWHM-D ~150 cm^{-1} and $I_D/I_G < 1$. The 2nd group contains the more mature chondrites, namely Grosnaja, Mokoia, Bali, Axtell, and Allende. They are characterised by FWHM-D < 105 cm^{-1} and $I_D/I_G > 1$. In the second group, the hierarchy in terms of maturation grade is unambiguous: Grosnaja < Mokoia ~ Bali < Axtell < Allende. On the other hand, it is difficult or even impossible to discriminate between the objects of the 1st group (Kaba, Vigarano, Efremovka, and Leoville): variations of I_D/I_G are large and without overlapping of the 1σ bars (except for Leoville and Vigarano), but FWHM-D mean values are very close. The parameters do not conflict but the two tracers do not exhibit the same sensitivity: FWHM-D seems to vary largely from Leoville to Mokoia/Bali and weakly down to Allende while I_D/I_G varies greatly from Mokoia/Bali to Allende. This may be explained by different sensitivities of the parameters to change of maturity.

The "D," "G," and "DG" diagrams (Fig. 2) clearly depict two groups: CV3s plot with the UOCs and can be easily distinguished from the coal standards. These observations suggest that OM in the two classes of chondrites are chemically close, and confirm the fact that coal samples cannot be considered as strictly valid analogues. The choice of humic coals was initially justified by their evolution over a long time scale, as well as by the similar chemical (H/C and O/C ratio) and structural characteristics (small lateral size of aromatic compounds) of chondrites and coals. But the D, G, and DG diagram of the present work clearly show that, even if the metamorphic pathways are comparable, the domain of variation of the spectral parameters is not the same for chondrites and coals.

4.2. Zoning of olivine phenocrysts

The thermal history of the CV3 chondrites must be assessed with independent tracers. In the present work, Raman spectroscopy provides the maturation grade of the OM, and finally its degree of heating as a result of the time–temperature history. However, no information is provided on where the heating occurred (solar nebula vs. parent body). The degree of heating experienced by the whole meteorite must be determined and compared with the maturation grade of OM to state whether or not the latter is a metamorphic tracer of the whole object. In the case of UOCs, such a comparison was straightforward given that reliable petrologic types were available (Quirico et al., 2003). For the CV3s studied here, the petrologic types are the subject of controversy. Another criteria was consequently used.

Thermal metamorphism on the parent body induces the progressive homogenisation and equilibration of mineral compositions throughout the objects. Olivine phenocrysts in type I chondrules are FeO-poor, show limited initial zoning and are particularly useful to detect Fe diffusion from the matrix into the chondrules. The degree of equilibration of Fe in these minerals was observed in BSE images (Fig. 7), and compositional profiles (Fig. 8) across the chondrule–matrix border were acquired for some objects. Note that the zoning length varies strongly from one chondrule to another and even within the same chondrule. This reveals the complexity of the physical parameters controlling diffusion: initial concentrations on both sides of the chondrule edge, texture, and composition of the matrix, mineral orientations, etc. The wide dispersion of zoning makes it difficult to quantitatively determine parameters such as temperature (e.g., Weinbruch et al., 1994). For this reason, we considered mainly the BSE images in this study, even though they provide only qualitative information. In order to increase the internal consistency of the data, only type I chondrules (FeO-poor; McSween, 1977) with a relatively constant environment (a minimum of opaque minerals and large olivine–matrix contacts) and composition (Porphyritic Olivine Pyroxene chondrules) were selected and only olivine grains in contact with matrix were considered.

A first set of measurements was composed of a series of UOCs with well known petrographic types (Sears et al., 1980; Sears et al., 1991b; Benoit et al., 2002): Semarkona (LL3.0), Bishunpur (LL3.1), Krymka (LL3.1), ALHA77176 (L3.2), ALH83010 (L3.3), Chainpur (L/LL3.4), Hallingeberg (L3.5), Tieschitz (H/L3.6), Parnallee (LL3.7), Villa Natamuros (L3.7), Dhajala (H3.8), and Bremervörde (H3.9). Thin sections were all supplied by the Museum National d'Histoire Naturelle (Paris, France).

In BSE images, no zoning of olivine phenocrysts is observed for objects of petrographic types ranging between 3.0 and 3.2 (Fig. 7a). Between types 3.4 and 3.7 (Figs. 7b and c), the formation of iron-rich olivine is systematic and the zoning increases progressively until equilibration in type 3.8 as for Dhajala (Fig. 7d). These observations are consistent with earlier results (see references within Brearley and Jones, 1998).

The same approach has been followed to study the zoning of olivine phenocrysts in the oxidised and reduced CV3 chondrites. BSE images depict two distinct groups: (1) Leoville, Vigarano, Efremovka, Kaba, and Bali and (2) Allende (Fig. 7e), Axtell (Fig. 7f), Mokoia (Fig. 7g) and Grosnaja (Fig. 7h). In the former, there is no evidence of the formation of iron-rich olivine, while in the latter the zoning of olivine phenocrysts is systematically observed. Compositional profiles across the chondrule–matrix edge reveal zoning up to 10 μm (Fig. 8) in Allende and Axtell and smaller zoning (a few μm) in Mokoia and Grosnaja. Chemical zoning depends on petrologic factors such as surrounding mineralogy or the initial FeO content. But it also depends, through the peak metamorphic temperature and cooling duration, on the thermal history of the parent body, during which the equilibration takes place. Thus it is not possible to define an absolute scale of zoning width for each petrologic type from UOCs, and to apply it to CV3s to determine their petrologic type. Nevertheless, the work on UOCs has shown that the zoning of olivine phenocrysts increases with petrologic type: the formation of iron-rich olivine seems to be linked with the thermal history. Thus, observations on BSE images for CV3s seem to indicate that Allende and Axtell are more metamorphosed than Mokoia and Grosnaja, which are more metamorphosed than the other CV3s, the reduced CV3s and Kaba.

5. Discussion

5.1. Maturation grade of organic matter as a tracer of thermal history

Maturation grade of OM and olivine zoning depict the two same main groups, except for Bali which will be discussed later. The good correlation between both these parameters suggests that thermal metamorphism on the parent body controls both the maturation of OM and Fe equilibration throughout the objects, as for the ordinary chondrites (McCoy et al., 1991). Nevertheless, these data need to be compared with other metamorphism tracers.

Noble gases are present in varying amounts in all chondritic meteorites. In ordinary chondrites, the petrographic type is correlated with their abundance (Marti, 1967; Heymann and Mazor, 1968). Mazor et al. (1970) reported a similar trend for the carbonaceous chondrites. A considerable number of new carbonaceous chondrites have been recently added to the noble gas database by Scherer and Schultz (2000), confirming the earlier results: the abundance of trapped noble gases in chondrites provides a strong indication of metamorphic history, with the most pristine having the highest gas contents. Noble gas data on bulk samples are available for five CV3 chondrites (Scherer and Schultz, 2000): Allende, Axtell, Bali, Grosnaja, and Mokoia. The rare gas contents are correlated with the degree of metamorphism as the concentrations of ^{84}Kr, ^{132}Xe, and ^{36}Ar are fairly well correlated with the Raman parameter FWHM-D (Fig. 9). This indicates that Allende is more metamorphosed than respectively Bali, Grosnaja, and Kaba. Axtell does not correlate very well with FWHM-D. Noble gas concentrations appear to be surprisingly low in comparison with those in Allende and Bali. Two explanations are possible: (1) a fluctuation due to a weight artefact. Indeed, bulk meteorite samples weighing only a few hundred milligram typically used for noble gas measurements (Huss and Lewis, 1994a,b), are not necessarily representative of the whole sample; (2) a possible effect of terrestrial weathering as Axtell is the only find in this series (Simon et al., 1995).

Nanodiamonds are the major carrier of noble gases. These five noble gases contain primarily three isotopic components (HL, P6 and P3; nomenclature in Huss and

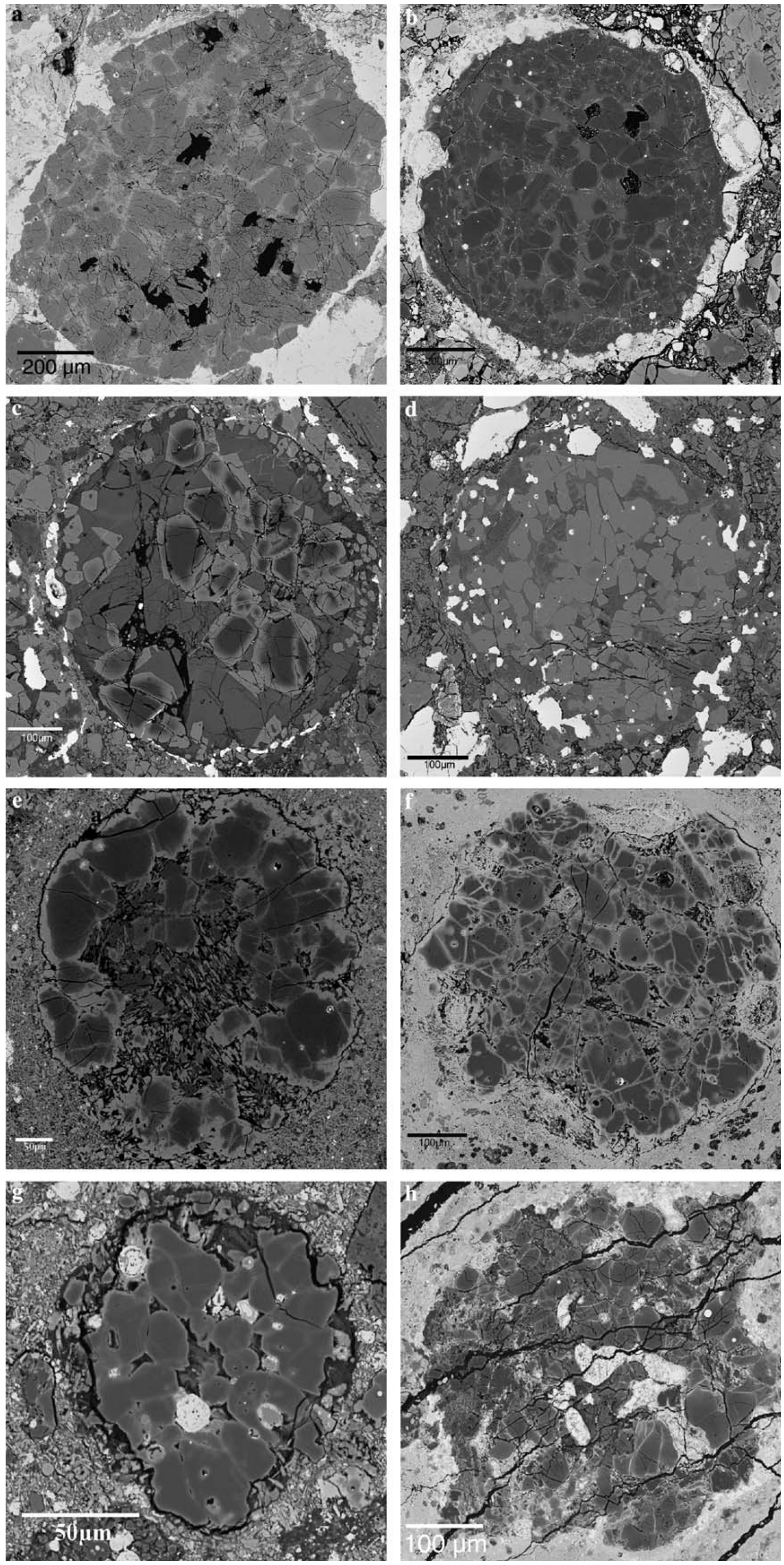

Fig. 7. SEM images of type I chondrules with olivine phenocrysts in contact with the surrounding matrix in UOCs (a, Semarkona (LL3.0), ×100; b, Chainpur (L/LL3.4), ×90; c, Villa Natamuros (L3.7), ×140; d, Dhajala (H3.8), ×150) and in CV3 chondrites (e, Allende, ×190; f, Axtell, ×150; g, Mokoia, ×370; h, Grosnaja, ×200). Figures a, b, c, and d show the increase in the zoning width with increasing petrologic type. Among the CV3s, the olivine phenocrysts of Allende, Axtell, Mokoia, and Grosnaja are systematically zoned. No zoning was observed for Efremovka, Leoville, Vigarano, Kaba, and Bali.

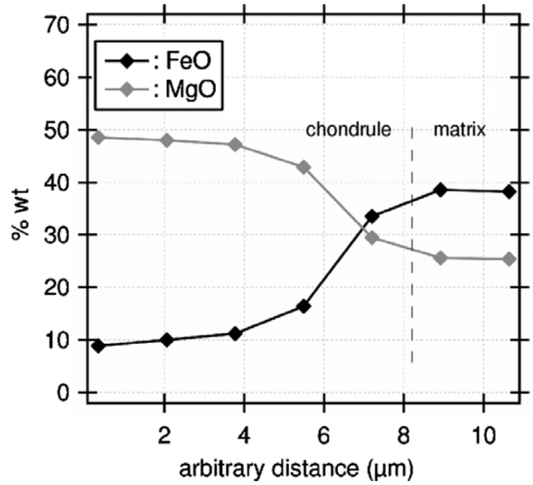

Fig. 8. Concentration profile across an iron-rich olivine phenocryst in a type I chondrule of Allende. Fe/Mg interdiffusion between the fayalite-rich rim and the forsterite core is limited to a few µm.

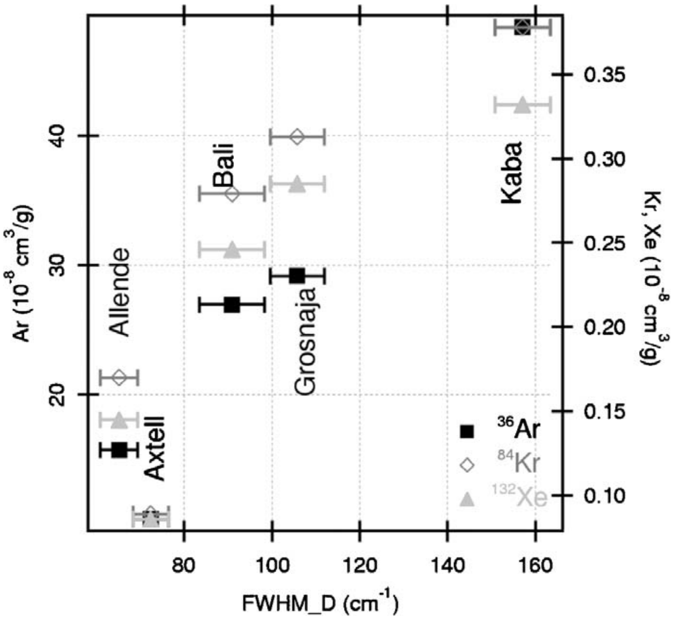

Fig. 9. Trapped planetary noble gases in oxidised CV3 chondrites vs. Raman spectral parameter FWHM-D. Noble gas data are from Scherer and Schultz (2000). Amounts of ^{36}Ar (black points), ^{84}Kr (grey points) and ^{132}Xe (light grey points) decrease as the metamorphic degree increases.

Lewis, 1994b). The P3 component has a solar isotopic abundance, is released at low temperature during the graphitisation of the host diamond, and its abundance reflects the degree of thermal metamorphism (Anders and Zinner, 1993; Huss and Lewis, 1994a,b, 1995). Its relative abundance in diamond samples can be understood in terms of thermal processing of a single mixture of diamonds such as those found in the unmetamorphosed CI and CM chondrites (Huss and Lewis, 1994b). These data support the evidence that Leoville is less metamorphosed than Vigarano and Allende. Plotting the abundance of the P3 component versus FWHM-D for these three CV3s and three UOCs (Fig. 10) reveals once again a good correlation. Russell et al. (1996) have shown that the C/N ratio and the δ^{13}C isotopic composition of nanodiamonds are partly controlled by thermal metamorphism. However, while the loss of noble gases is mostly controlled by temperature, other factors such as the mineralogical composition also control the loss of nitrogen through oxidation processes. These data do not suggest a clear metamorphic hierarchy between Allende, Efremovka, and Vigarano, which is likely a consequence of the variations in the mineralogical composition of these objects.

The abundance of presolar grains (normalised to matrix) is also controlled by the metamorphic history of the host meteorite (Alexander et al., 1990; Huss, 1990; Huss and Lewis, 1994a,b). Within a meteorite class, the abundances of presolar grains correlate with the petrologic type (Huss and Lewis, 1995). Data on nanodiamonds (Table 3) are available for Allende, Vigarano, and Leoville. They show that Allende may have undergone more metamorphism than Vigarano and Leoville.

The order of increasing metamorphism as reflected by the maturation grade of the OM is thus consistent with that given by several other independent tracers. All these tracers but one deal with OM or compounds inside OM. They show that the organic matter and their host phases have experienced similar thermal events and therefore were likely already associated prior to this event. The zoning of olivine phenocrysts reflects thermal metamorphism as experienced by the whole rock. The maturation grade of OM as revealed by Raman spectroscopy correlates with all these tracers and can be considered as a reliable indicator of thermal metamorphism of the whole rock. Moreover, the consistency of the results support the evidence that the OM precursors and metamorphic conditions among the studied CV3s are rather similar.

Bali is an exception. The maturation grade of its OM ranges between those of Grosnaja and Axtell (Fig. 4), which is consistent with bulk noble gas abundance (Scherer and Schultz, 2000). However, no zoning was visible on its olivine phenocrysts. Bali is known to be heterogeneous, in particular with coexisting highly and poorly altered regions (Keller et al., 1994; Brearley and Jones, 1998). It is obvious that a microbeam technique like Raman spectroscopy might suffer from artefacts due to heterogeneity, and it is likely that the raw samples measured by Raman spectroscopy and the polished sections studied by BSE imaging have distinct metamorphism grades. For Bali, a metamorphism grade should be provided for each clast of the meteorite. Unfortunately, this is not possible as it would require surveying a large number of thin sections and raw samples. Our study points to the presence of at least two clasts with a low and a high metamorphism grade, and at last provides a quantitative estimation of the high grade. For all other CV chondrites studied here, the consistency of all metamorphism tracers suggests a single metamorphism grade for each chondrite and shows that the small number of measurements does not result in misleading conclusions.

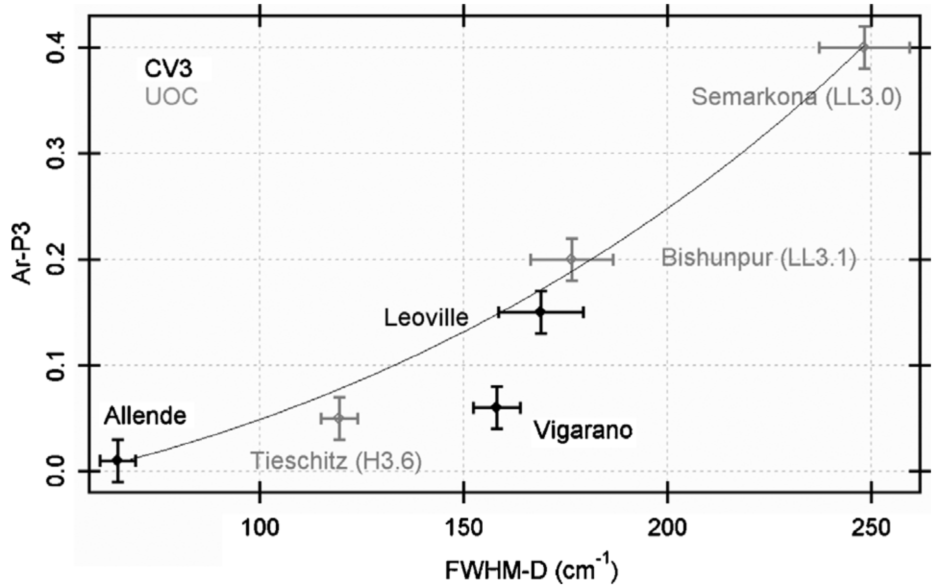

Fig. 10. Isotopically "normal" P3 noble-gas components vs. Raman spectral parameter FWHM-D (cm^{-1}) of CV3s (black points) and UOCs (grey points). The values decrease with increasing degree of metamorphism (from Anders and Zinner, 1993).

Table 3
Diamond abundance for bulk meteorites

Type	Meteorite	Matrix normal (ppm)[a]
CV3s	Vigarano	1806
	Leoville	1554
	Allende	885

[a] Diamond abundances for bulk meteorites calculated from Ne-A2 supported Xe-HL in etched residues using Xe-HL abundances from diamond separates; value normalised with respect to Orgueil matrix, from Huss and Lewis (1995).

The small number of measurements is nevertheless a key problem as it is not clear whether the 1σ dispersion in the Raman tracers is related to the measurement uncertainty or structural variations of the IOM on a micrometric scale. The variations of the FWHM-D and I_D/I_G parameters in the group of the less metamorphosed CV3s (see Section 4.1) may be due to OM heterogeneity. Improving the accuracy and reproducibility of such measurements is certainly a key objective for future studies (Beyssac et al., 2003; Quirico et al., 2005).

To summarise, CV3 chondrites represent a large metamorphic sequence and are not systematically primitive objects. The following hierarchy, based on Raman measurements and validated by several independent tracers, is suggested: Allende > Axtell > Bali ~ Mokoia > Grosnaja ≫ Efremovka > Vigarano ~ Leoville > Kaba.

5.2. *Attribution of petrologic types to CV3s by comparison with UOCs*

Raman data are consistent with the accretion of close organic precursors by UOCs and CV chondrites. It is therefore possible to propose a set of petrologic types as defined for UOCs (Quirico et al., 2003). The Raman parameters FWHM-D and I_D/I_G for the nine CV3s and six ordinary chondrites (see Section 3.3 and Section 4.1) can be used for interclass comparison (Fig. 4). In terms of FWHM-D, Allende is comparable with Parnallee (LL3.7); Grosnaja, Bali, Mokoia, and Axtell range between Tieschitz (H/L3.6) and Parnallee (LL3.7); Vigarano, Kaba, and Efremovka range between Krymka (LL3.1) and Chainpur (L/LL3.4); Leoville is comparable with Krymka (LL3.1). In terms of I_D/I_G, Grosnaja, Mokoia, Bali, Axtell, and Allende range between Tieschitz (H/L3.6) and Parnallee (LL3.7); Efremovka ranges between Chainpur (L/LL3.4) and Krymka (LL3.1) which is comparable with Bishunpur, Vigarano and Leoville. Kaba is slightly smaller than Semarkona (LL3.0). The following constraints on the petrographic types (PT) are then deduced (Table 4). Bali, Axtell and Allende are the most metamorphosed CV3s with PT > 3.6. Mokoia and Grosnaja are also significantly metamorphosed but to a lesser extent, with a suggested PT ~3.6. Vigarano, Leoville, and Efremovka are less metamorphosed with PTs ranging between type 3.1 and 3.4. Last, Kaba appears as the most pristine object with PT = 3.1.

In the previous section, the P3 component introduced by Huss and Lewis (1994b) was used to demonstrate that the OM maturation reflects the degree of thermal metamorphism. This metamorphism tracer is of special interest because it does not depend on the mineralogical composition and therefore on the chemical class of the chondrites. It can therefore be used for cross-calibration of various scales of petrologic type, under the assumption that all classes inherited the same mixture of primitive diamonds (Alexander et al., 1998; Huss and Lewis, 1994b). P3 concentrations are provided for three CV3s and three UOCs (Fig. 9). They indicate Allende with PT > 3.6, Vigarano with $3.4 \leqslant PT \leqslant 3.6$ and Leoville with $3.2 \leqslant PT \leqslant 3.4$. These results are consistent with the Raman results. They support

Table 4
Comparison of attributed petrologic type

Meteorite[a]	FWHM-D[b] (cm^{-1})	I_D/I_G[c]	TL sensitivities (~250 °C) Dhajala = 1[d]	Proposed PT[e] This work	Proposed PT[e] ITL[d]
Allende (O, F)	65 ± 4	1.54 ± 0.06	0.012 ± 0.001	>3.6	3.2
Axtell (O, f)	72 ± 4	1.42 ± 0.04	—	>3.6	3.0
Bali (O, F)	91 ± 7	1.19 ± 0.08	0.11 ± 0.06	>3.6	3.0
			0.15 ± 0.07		
Mokoia (O, F)	89 ± 8	1.13 ± 0.08	0.018 ± 0.001	~3.6	3.2
			0.005 ± 0.001		
Grosnaja (O, F)	106 ± 6	1.05 ± 0.04	0.011 ± 0.004	~3.6	3.3
			0.009 ± 0.002		
Efremovka (R, f)	158 ± 13	1.00 ± 0.03	0.051 ± 0.003	3.1–3.4	3.2
			0.032 ± 0.01		
Vigarano (R, F)	158 ± 6	0.94 ± 0.02	0.06 ± 0.01	3.1–3.4	3.3
			0.047 ± 0.006		
Leoville (R, f)	169 ± 10	0.94 ± 0.03	0.94 ± 0.26	3.1–3.4	3.0
			2.8 ± 0.2		
Kaba (O, F)	157 ± 6	0.83 ± 0.02	0.62 ± 0.19	3.1	3.0
			0.84 ± 0.11		

[a] O, oxidised; R, reduced; F, fall; and f, find.
[b] FWHM-D: band width of the Raman D-band.
[c] I_D/I_G: peak intensity ratio of the Raman D- and G-bands.
[d] Guimon et al. (1995).
[e] PT, petrographic type.

evidence that the Raman approach is reliable for determining the petrographic type of the CV3 chondrites.

Comparison with the widely used Induced ThermoLuminescence (ITL) technique reveals large differences between petrographic type attributions (Guimon et al., 1995; Table 4). The present results, crossed with independent tracers from earlier works, show that ITL provides erroneous petrographic types. The differences between the determined petrographic types are weaker for reduced than for oxidised CV3s. The ITL signal originates from the feldspar formed by the devitrification of mesostasis glass during metamorphism (Sears et al., 1980; Brearley and Jones, 1998; Benoit et al., 2002), and was initially developed on Ordinary Chondrites that suffered weak or negligible aqueous alteration (Grossman et al., 2000). On the other hand, oxidised CV3 chondrites suffered major aqueous alteration that led to dissolution of mesostasis glass and feldspars, explaining why the petrologic subtypes of these objects are systematically underestimated. Moreover, the calibration between TL sensitivity and metamorphism is not the same for all chondrite classes. The TL sensitivity range for CV3 chondrites (Guimon et al., 1995) is the same as those proposed for CO chondrites (Sears et al., 1991b) but is different from those proposed for the UOCs (Sears et al., 1991b). Thus TL sensitivity cannot be used to propose an interclass comparison with UOCs.

5.3. Nebular or asteroidal records in CV chondrites?

McSween (1977) first pointed out that CVs exhibit larger mineralogical and petrologic variations than any other chondrite class. These variations may be the result of asteroidal processes. Unlike most other chondrites, CV chondrites experienced various degrees of thermal metamorphism and aqueous alteration, with some objects such as Allende having experienced high degrees of both processes. Krot et al. (1995) and Kojima and Tomeoka (1996) have suggested that much petrologic and mineralogical information interpreted as nebular records might have an asteroidal origin.

Fe zoning in chondrules has been explained either by interdiffusion between chondrules and nebular gas (Peck and Wood, 1987; Hua et al., 1988; Ikeda and Kimura, 1995, 1996; Kimura and Ikeda, 1997) or by interdiffusion on the parent body due to thermal metamorphism (Housley and Cirlin, 1983; Housley, 1986; Krot et al., 1995; Kojima and Tomeoka, 1996). Many studies have focused exclusively on Allende. Studies which consider series of CVs observe variations in the extent of zoning from one object to another. Peck and Wood (1987) report the absence of zoning in Kaba and Vigarano, and weak zoning in Mokoia and Grosnaja. Kimura and Ikeda (1997) report systematic measurements on 10 chondrules in Efremovka, Vigarano and Leoville and the following hierarchy in chondrule zoning: Leoville < Efremovka < Vigarano < Allende. These results are fairly consistent with ours. Considering a series of CV chondrites with different metamorphism grades shows that the observed zonings reported in the literature are correlated to the degree of thermal metamorphism, suggesting that these features are induced by thermal metamorphism and should be no longer considered as nebular records.

Fe-rich fayalite in matrix has been interpreted as the result of nebular condensation (Hua and Buseck, 1995; Weisberg and Prinz, 1998). These conclusions have been applied to many CVs without considering the importance of asteroidal processes. In particular, the role of aqueous alteration has been underestimated. Weinbruch et al. (1990) argued that equilibration between chondrules and adjacent minerals from the matrix in Allende did not occur on the parent body because they were not locally equilibrated. There are other possible explanations. Aqueous alteration may redistribute elements like Fe throughout the matrix, and neoformed olivine grains with a large range of compositions, including Fe-rich phases, may form by dehydration. This explanation supports petrologic evidence (Krot et al., 1997) and thermodynamic calculations that have recently demonstrated that fayalite can form on a CV3 parent body under aqueous alteration conditions (Zolotov et al., 2005). The range of composition of olivine grains in matrix (Krot et al., 1995) is therefore not only controlled by thermal metamorphism, but also by the extent of aqueous alteration and by the timing of the latter with respect to the peak metamorphism event. In Bali, aqueously altered clasts exhibit a wide compositional range of olivine grains, whereas the distribution is rather narrow in anhydrous clasts (Keller et al., 1994). Mokoia also exhibits a wide compositional range (Cohen et al., 1983), close to Kaba, but its metamorphism grade is close to that of the oxidised Grosnaja (PT ~3.6). The compositional range of olivine grains here provides clues on the timing of both asteroidal processes: in Mokoia, aqueous alteration postdates the metamorphism peak whereas in Grosnaja, all hydrated minerals were dehydrated and transformed due to thermal metamorphism, with a subsequent reequilibration. This scenario is consistent with the high phyllosilicate abundance in Mokoia (Tomeoka and Buseck, 1990).

Finally, assessing the degree of metamorphism grade independently from aqueous alteration and from the mineralogical context enhances the understanding of the petrology and mineralogy of CV3 chondrites. The effect of both high degrees of thermal metamorphism and aqueous alteration should be considered in the future to provide a better understanding of parent body asteroidal processes. Less metamorphosed objects should also be studied, and in particular, Allende should be avoided in studies concerned with primary nebular processes. To sum up, it is worth citing the conclusions of Kojima and Tomeoka (1996): "If our view is correct, it may be necessary to reevaluate much of the previous interpretations of the origin and the formation process of CV chondrites which have overwhelmingly emphasised primary nebular processes".

5.4. Origin and evolution of OM in CV3s

The use of the maturation grade of OM as a metamorphic tracer requires similar organic precursors to have been accreted by all the parent bodies. This statement is supported by the correlation between the Raman parameters and independent metamorphism tracers, as well as the close vicinity of the data points in the so-called G, D, and DG diagrams. These results support the suggestion of Alexander et al. (1998) that all chondrites accreted similar OM precursors, based mainly on the isotopic composition of IOM and nanodiamond abundance. Nevertheless, insufficient quantitative structural and chemical data on the IOMs is available to draw firm conclusions. Although it is likely true that the precursors are chemically and structurally similar, it is very unlikely that they are exactly the same. Some differences in the elemental and isotopic compositions of the IOMs as well as in their microtextures, largely controlled by precursor and metamorphic conditions, should, when considered along with the maturity, provide more accurate constraints on this hypothesis.

Quirico et al. (2003) have also discussed the possible role of water in the maturation rate of OM. The present study, considering both aqueously unaltered and heavily aqueously altered objects shows that the role of water in the maturation grade of OM is extremely weak or negligible in this metamorphic range.

6. Conclusion

The present study focused on the maturation grade of organic matter to investigate the thermal history of a series of CV3 chondrites. The main results are the following:

(1) The petrologic types of a series of CV chondrites have been re-analysed leading to the following attribution: PT(Allende-Axtell) > 3.6; PT (Bali-Mokoia-Grosnaja) ~3.6; PT (Efremovka-Leoville-Vigarano): 3.1–3.4; PT (Kaba) ~3.1. The most studied CV3, Allende, is the most metamorphosed. Bali is a breccia containing clasts of different petrologic types. The attribution suggested by this study is that of clasts of the highest petrologic types, as pointed by IOM maturity and noble gas bulk abundance.

(2) The maturity of IOM as controlled by thermal metamorphism supports evidence that the organic precursors accreted by UOCs and CV chondrites were chemically similar, though it is unlikely they were exactly the same. Water has no or a negligible action in the thermal metamorphism process.

(3) CV3s are complex objects which have experienced various degrees of thermal metamorphism and aqueous alteration, resulting in complex mineralogical and petrologic characteristics. As a consequence, evidence of nebular records reported in the literature, such as chondrule chemical zoning (exchange between nebular gas and chondrules) or fayalite grains (direct condensation from nebular gas), can be explained by asteroidal processes.

(4) The range of composition of olivine grains in matrix does not mirror the metamorphism grade if subsequent aqueous alteration occurred after the metamorphism peak. This is the case for Mokoia, exhibiting an olivine composition range similar to that of Kaba but with a metamorphism grade close to that of Grosnaja (PT: 3.6).

Acknowledgments

We thank Dr. Monica M. Grady (Natural History Museum, London), Dr. Glen MacPherson (US National Museum of Natural History, Washington), Dr. Gero Kurat (Naturhistorisches Museum, Vienna), Dr. Meenakshi Wadhwa (Field Museum Of Natural History, Chicago) and Dr. B. Zanda (Museum National d'Histoire Naturelle, Paris) for providing us with precious meteorite samples. S. Krot is warmly thanked for valuable discussions on asteroidal processes in CV parent bodies. We are very grateful to S. Russell and B. Wopenka for pertinent comments and suggestions that greatly improved the manuscript. We also thank M. Sephton for an interesting and positive review of this manuscript. This work has been funded by the Centre National d'Etudes Spatiales (CNES-France).

Associate editor: Sara S. Russell

References

Alexander, C.M.O.'D, Barber, D.J., Hutchison, R., 1989. The microstructure of Semarkona and Bishunpur. *Geochim. Cosmochim. Acta* **53**, 3045–3057.

Alexander, C.M.O.'D., Arden, J.W., Ash, R.D., Pillinger, C.T., 1990. Presolar components in the ordinary chondrites. *Earth Planet. Sci. Lett.* **99**, 220–229.

Alexander, C.M.O'D., Russell, S.S, Arden, J.W., Ash, R.D., Grady, M.M., Pillinger, C.T., 1998. The origin of chondritic macromolecular organic matter: a carbon and nitrogen isotope study. *Meteorit. Planet. Sci.* **33**, 603–622.

Anders, E., Zinner, E., 1993. Interstellar grains in primitive meteorites—diamond, silicon carbide, and graphite. *Meteoritics* **28**, 490–514.

Benoit, P.H., Akridge, G.A., Ninagawa, K., Sears, D.W.G., 2002. ThermoLuminescence sensitivity and thermal history of type 3 ordinary chondrites: eleven new type 3.0–3.1 chondrites and possible explanations for differences among H, L and LL chondrites. *Meteorit. Planet. Sci.* **37**, 793–805.

Beny-Bassez, C., Rouzaud, J.N., 1985. Characterization of carbonaceous materials by correlated electron and optical microscopy and Raman microspectroscopy. In: *Scanning Electron Microscopy*, SEM Inc. AMF O'Hare, Chicago, 119–132.

Beyssac, O., Rouzaud, J.N., Goffé, B., Brunet, F., Chopin, C., 2002. Graphitization in a high-pressure, low-temperature metamorphic gradient: a Raman microspectrometry and HRTEM study. *Contrib. Mineral. Petrol.* **143**, 19–31.

Beyssac, O., Goffé, B., Petitet, J.-P., Froigneux, E., Moreau, M., Rouzaud, J.-N., 2003. On the characterization of disordered and heterogeneous carbonaceous materials by Raman spectroscopy. *Spectrochim. Acta A* **59**, 2267–2276.

Brearley A.J., Jones R.H., 1998. Chondritic Meteorites. In: Papike, J.J. (Ed.), *Planetary Materials*. Mineralogical Society of America, pp. 3.220–225, 3.52–63.

Cohen, R.E., Kornacki, A.S., Wood, J.A., 1983. Mineralogy and petrology of chondrules and inclusions in the Mokoia CV3 chondrite. *Geochim. Cosmochim. Acta* **47**, 1739–1757.

Everall, N.J., Lumsdon, J., Christopher, D.J., 1991. The effect of laser-induced heating upon the vibrational Raman spectra of graphites and carbon fibres. *Carbon* **29** (2), 133–137.

Ferrari, A.C., Robertson, J., 2000. Interpretation of Raman spectra of disordered and amorphous carbon. *Phys. Rev. B* **61** (20), 14095–14107.

Grossman, J.N., 2004. Loss of chromium from olivine during the metamorphism of chondrites. *Lunar Planet. Sci*. XXXV. Lunar Planet. Inst., Houston. #1320 (abstr.).

Grossman, J.N., Alexander, C.M.O'D, Wang, J., Brearley, A., 2000. Bleached chondrules: evidence for widespread aqueous processes on the parent asteroids of ordinary chondrites. *Meteorit. Planet. Sci.* **35**, 467–486.

Guimon, R.K., Symes, S.J.K., Sears, D.W.G., Benoit, P.H., 1995. Chemical and physical study of type 3 chondrites XII: the metamorphic history of CV chondrites and their components. *Meteoritics* **30**, 704–714.

Heymann, D., Mazor, E., 1968. Noble gases in unequilibrated ordinary chondrites. *Geochim. Cosmochim. Acta* **32**, 1–19.

Housley, R.M., 1986. Possible CV Parent Body Alteration Processes. *Lunar Planet. Sci.* XVII, Lunar Planet. Inst., Houston. pp. 366–367 (abstr).

Housley, R.M., Cirlin, E.H., 1983. On the alteration of allende chondrules and the formation of matrix. In: King, E.A. (Ed.), *Chondrules and their Origin*. Lunar and Planetary Institute, Houston, pp. 145–161.

Hua, X., Buseck, P.R., 1995. Fayalite in the Kaba and Mokoia carbonaceous chondrites. *Geochim. Cosmochim. Acta* **59**, 563–578.

Hua, X., Adam, J., Palme, H., El Goresy, A., 1988. Fayalite-rich rims, veins, and halos around and in forsteritic olivines in CAIs and chondrules in carbonaceous chondrites: types, compositional profiles and constraints of their formation. *Geochim. Cosmochim. Acta* **52**, 1389–1408.

Huss, G.R., 1990. Ubiquitous interstellar diamond and SiC in primitive chondrites: abundances reflect metamorphism. *Nature* **347**, 159–162.

Huss, G.R., Lewis, R.S., 1994a. Noble gases in presolar diamonds I: three distinct components and their implications for diamonds origins. *Meteoritics* **29**, 791–811.

Huss, G.R., Lewis, R.S., 1994b. Noble gases in presolar diamonds II: component abundances reflect thermal processing. *Meteoritics* **29**, 811–829.

Huss, G.R., Lewis, R.S., 1995. Presolar diamond, SiC and graphite in primitive chondrites: abundance as a function of meteorite class and petrologic type. *Geochim. Cosmochim. Acta* **59** (1), 115–160.

Huss, G.R., Lewis, R.S., Hemkin, S., 1996. The "normal planetary" noble gas component in primitive chondrites: compositions, carrier, and metamorphic history. *Geochim. Cosmochim. Acta* **60** (17), 3311–3340.

Ikeda, Y., Kimura, M., 1995. Anhydrous alteration of Allende chondrules in the solar nebula I: description and alteration of chondrules with known oxygenisotopic compositions. *Proc. NIPR Symp. Antarct. Meteorit.* **8**, 97–122.

Ikeda, Y., Kimura, M., 1996. Anhydrous alteration of Allende chondrules in the solar nebula III: alkali-zoned chondrules and heating experiments for anhydrous alteration. *Proc. NIPR Symp. Antarct. Meteorit.* **9**, 51–68.

Kelemen, S.R., Fang, H.L., 2001. Maturity trends in Raman spectra from kerogen and coal. *Energy Fuel* **15**, 653.

Keller, L.P., Buseck, P.R., 1990. Aqueous alteration in the Kaba CV3 carbonaceous chondrite. *Geochim. Cosmochim. Acta* **54**, 2113–2120.

Keller, L.P., McKay, D.S., 1993. Aqueous alteration of the Grosnaja CV3 carbonaceous chondrite. *Meteorit. Planet. Sci.*. Abstract # 378.

Keller, L.P., Thomas, K.L., Clayton, R.N., Mayeda, T.K., DeHart, J.M., McKay, D.S., 1994. Aqueous alteration of the Bali CV3 chondrite: evidence from mineralogy, mineral chemistry, and oxygen isotopic compositions. *Geochim. Cosmochim. Acta* **58** (24), 5589–5598.

Kimura, M., Ikeda, Y., 1997. Comparative study of anhydrous alteration of chondrules in reduced and oxidized CV chondrites. *Antarct. Meteorit. Res.* **10**, 191–202.

Kojima, T., Tomeoka, K., 1996. Indicators of aqueous alteration and thermal metamorphism on the CV parent body: microtextures of a dark inclusion from Allende. *Geochim. Cosmochim. Acta* **60** (14), 2651–2666.

Krot, A.N., Scott, E.R.D., Zolensky, M.E., 1995. Mineralogical and chemical modification of components in CV3 chondrites: nebula or asteroidal processing? *Meteoritics* **30**, 748–775.

Krot, A.N., Scott, E.R.D., Zolensky, M.E., 1997. Origin of fayalitic olivine rims and lath-shaped matrix olivine in the CV3 chondrite Allende and its dark inclusions. *Meteorit. Planet. Sci.* **32**, 31–49.

Krot, A.N., Petaev, M.J., Scott, E.R.D., Choi, B.G., Zolensky, M.E., Keil, K., 1998. Progressive alteration in CV3 chondrites: more evidence for asteroidal alteration. *Meteorit. Planet. Sci.* **33**, 1065–1085.

Marti, K., 1967. Trapped xenon and the classification of chondrites. *Earth Planet. Sci. Lett.* **2**, 193–196.

Mazor, E., Heymann, D., Anders, E., 1970. Noble gases in carbonaceous chondrites. *Geochim. Cosmochim. Acta* **34**, 781–824.

McCoy, T.J., Scott, E.R.D., Jones, R.H., Keil, K., Taylor, G.J., 1991. Composition of chondrule silicates in LL3-5 chondrites and implications for their nebular history and parent body metamorphism. *Geochim. Cosmochim. Acta* **55**, 601–619.

McSween, H.Y., 1977. Petrographic variations among carbonaceous chondrites of the Vigarano type. *Geochim. Cosmochim. Acta* **41**, 1777–1790.

Peck, J.A., Wood, J.A., 1987. The origin of ferrous zoning in Allende chondrule olivines. *Geochim. Cosmochim. Acta* **51**, 1503–1510.

Pradier, B., Landais, P., Rochdi, A., Davis, A., 1992. Chemical basis of fluorescence alteration of crude oils and kerogens—II. Fluorescence and infrared micro-spectrometric analysis of vitrinite and liptinite. *Org. Geochem.* **18**, 241–248.

Quirico, E., Raynal, P.I., Bourot-Denise, M., 2003. Metamorphic grade of organic matter in six unequilibrated ordinary chondrites. *Meteorit. Planet. Sci.* **38** (5), 795–811.

Quirico, E., Rouzaud, J.N., Bonal, L., Montagnac, G., 2005. Maturation grade of coals as revealed by Raman spectroscopy: progress and problems. *Spectrochim. Acta A* **61**, 2368–2377.

Russell, S.S, Arden, J.W., Pillinger, C.T., 1996. A carbon and nitrogen isotope study of diamond from primitive chondrites. *Meteorit. Planet. Sci.* **31**, 343–355.

Scherer, P., Schultz, L., 2000. Noble gas record, collisional history, and pairing of CV, CO, CK, and other carbonaceous chondrites. *Meteorit. Planet. Sci.* **35**, 145–153.

Sears, D.W.G., Hasan, F.A., Batchelor, J.D., Lu, J., 1983. Chemical and physical studies of type 3 chondrites—metamorphism, pairing and brecciation of ordinary chondrites. *Proc. Lunar Planet. Sci. Conf.* **21**, 493–512.

Sears, D.W.G., Batchelor, J.D., Lu, J., Keck, B.D., 1991b. Metamorphism of CO and CO-like chondrites and comparisons with type 3 ordinary chondrites. *Proc. NIPR Symp. Antarct. Meteorit.* **4**, 319–343.

Sears, D.W.G., Grossman, J.N., Melcher, C.L., Ross, L.M., Mills, A.A., 1980. Measuring metamorphic history of unequilibrated ordinary chondrites. *Nature* **287**, 791–795.

Simon, S.B., Grossman, L., Casanova, I., Symes, S., Benoit, P., Sears, D.W.G., Wacker, J.F., 1995. Axtell, a new CV3 chondrite find from Texas. *Meteoritics* **30**, 42–47.

Tomeoka, K., Buseck, P.R., 1990. Phyllosilicates in the Mokoia CV carbonaceous chondrite: evidence for aqueous alteration in an oxidizing environment. *Geochim. Cosmochim. Acta* **54**, 1745–1754.

Tomeoka, K., Tanimura, I., 2000. Phyllosilicate-rich chondrule rims in the vigarano cv3 chondrite: evidence for parent-body processes. *Geochim. Cosmochim. Acta* **64**, 1971–1988.

Tuinstra, F., Koenig, J.L., 1970. Raman spectrum of graphite. *J. Chem. Phys.* **53**, 1126–1130.

Weinbruch, S., Armstrong, J., Palme, H., 1994. Constraints on the thermal history of the Allende parent body as derive from olivine-spinel thermometry and Fe/Mg interdiffusion in olivine. *Geochim. Cosmochim. Acta* **58** (2), 1019–1030.

Weinbruch, S., Palme, H., Müller, W.F., El Goresy, A., 1990. FeO-rich rims and veins in Allende forsterite: evidence for high temperature condensation at oxidizing conditions. *Meteoritics* **25**, 115–125.

Weisberg, M.K., Prinz, M., 1998. Fayalitic olivine in CV3 chondrite matrix and dark inclusions: a nebular origin. *Meteorit. Planet. Sci.* **33**, 1087–1099.

Weisberg, M.K., Prinz, M., Clayton, R.N., Mayeda, T.K., 1997. CV3 chondrites: three subgroups, not two. *Meteorit. Planet. Sci.* **32** (4), A138–A139.

Wopenka, B., Pasteris, J.D., 1993. Structural characterization of kerogens to granulite-facies graphite: Applicability of Raman microprobe spectroscopy. *Am. Mineral.* **78**, 533–557.

Zolotov, M.Yu., Mironenko, M.V., Schock, E.L., 2005. Thermodynamics constrains on fayalite formation on parent bodies of chondrites. *Meteorit. Planet. Sci.* **40**, A175. Asbtract # 5074.